The Journal of Experimental Biology 213, 1301-1308

doi:10.1242/jeb.039305

Activity, abundance, distribution and expression of Na^+/K^+-ATPase in the salt glands of *Crocodylus porosus* following chronic saltwater acclimation

Rebecca L. Cramp[1], Nicholas J. Hudson[2] and Craig E. Franklin[1,*]

[1]School of Biological Sciences, The University of Queensland, Brisbane, QLD 4072, Australia and [2]CSIRO Livestock Industries, Queensland Bioscience Precinct, St Lucia, QLD 4067, Australia

*Author for correspondence (c.franklin@uq.edu.au)

Accepted 5 January 2010

SUMMARY

Saltwater crocodiles, *Crocodylus porosus*, possess lingual salt glands which function to remove excess Na^+ and Cl^- accumulated as a consequence of living in salt water. Little is known about the nature of ion transport systems in *C. porosus* salt glands and how these systems respond to an osmotic challenge. In the present study, we examined the distribution and regulation of the Na^+/K^+-ATPase (NKA) pump, specifically the α-(catalytic) subunit in the salt glands of *C. porosus* chronically acclimated (6 months) to freshwater (FW) or 70% seawater (SW). We hypothesised that in the SW-acclimated *C. porosus* there would be an up-regulation of the abundance, activity and gene expression of the NKA transporter. NKA was immunolocalised to the lateral and basal membrane of secretory cells. As predicted, the NKA α-subunit was 2-fold more abundant in SW-acclimated *C. porosus* salt glands. NKA gene expression was also elevated in the salt glands of SW- *vs* FW-acclimated crocodiles. There was no increase in the specific activity of NKA in SW-acclimated animals and the *in vitro* rate of oxygen consumption by salt gland slices from SW-acclimated animals was not significantly different from that of FW-acclimated animals. The proportion of tissue oxygen consumption rate attributable to NKA activity was not different between SW- and FW-acclimated animals (approximately 50%). These data suggest that either chronic SW acclimation does not affect NKA in crocodile salt glands in the same manner as seen in other models or crocodiles possess the capacity to moderate NKA activity following prolonged exposure to SW.

Key words: acclimation, lingual salt gland, osmoregulation, reptile.

INTRODUCTION

Many marine non-mammalian vertebrates utilise specialised extra-renal salt-secreting tissues (salt glands) to assist in the removal of excess sodium and chloride ions. Marine birds utilise orbital salt glands (Schmidt-Nielsen, 1960), turtles have lachrymally located salt glands (Schmidt-Nielsen and Fänge, 1958), sea snakes have sublingual salt glands (Taub and Dunson, 1967; Dunson, 1968) and crocodiles have lingual salt glands (Taplin and Grigg, 1981). Similarly, elasmobranchs utilise rectal glands for salt excretion (Bulger, 1963). The morphology of these salt-secreting glands is highly conserved (Kirschner, 1980). Most are typically classified as compound, tubular structures; they are highly vascularised and densely innervated. Salt gland tubules consist of numerous highly modified secretory cells, which are characterised by their highly amplified basolateral membrane surface area. The basolateral membranes of salt gland secretory cells are closely apposed to surrounding capillary networks. The much smaller apical surface provides an interface between the cell and the secretory tubule lumen. These tissues are typified by their abundance of ion pumps, including Na^+/K^+-ATPase (NKA), a basolateral, transmembrane ion pump responsible for the maintenance of cellular electrochemical gradients through the movement of Na^+ and K^+ ions against their osmotic gradients. NKA is consistently present in large amounts in salt gland tissues specialised for active ion transport (Dunson and Dunson, 1975). Indeed, avian salt glands and elasmobranch rectal glands have become important model tissues for studies of the role of NKA in active ion transport.

The current model of ion secretion by salt gland cells suggests that the secretory cells' basolateral membrane contains numerous electrogenic NKA pumps which provide the driving force for the active secretion of Cl^-. Basolateral Na^+–K^+–$2Cl^-$-co-transporters (NKCC) are responsible for the active uptake of chloride ions from the blood, while cystic fibrosis transmembrane conductance regulator (CFTR)-like Cl^- transporters are responsible for the secretion of Cl^- across the apical membrane. Na^+ and K^+ gradients are actively maintained by basolateral NKA and NKCC pumps and K^+ channels, while Na^+ secretion occurs *via* ion-selective paracellular channels in apical tight junctions using the electrochemical gradient generated by the active secretion of Cl^- from the apical membrane (reviewed by Shuttleworth and Hildebrandt, 1999).

Salt glands are highly plastic tissues – both morphologically and functionally. Acute exposure to hypersaline drinking water results in rapid increases in gland size and secretory rate in domestic ducks (Schmidt-Nielsen and Kim, 1964). During chronic saltwater exposure, avian salt gland secretory cells undergo hypertrophy as well as hyperplasia (Knight and Peaker, 1979; Bentz et al., 1999). In addition, NKA activity and expression increase almost 2-fold within as little as 24 h (Fletcher et al., 1967; Hildebrandt, 1997). Similar changes in secretory cell size and NKA activity and expression have also been observed in elasmobranch and teleost models (Piermarini and Evans, 2000; Scott et al., 2004; Pillans et al., 2005; Evans, 2008).

The saltwater crocodile, *Crocodylus porosus*, possesses lingual salt glands which function to remove excess Na^+ and Cl^- ions accumulated as a consequence of living in marine environments (Taplin and Grigg, 1981). Saltwater crocodiles display a remarkable degree of euryhalinity; animals have been found to successfully

osmoregulate in salinities ranging from 0 to 60‰ (Grigg et al., 1986). Like avian salt glands, chronic exposure to hypersaline water results in an increase in *C. porosus* salt gland size and Na^+ secretion capacity (Cramp et al., 2007; Cramp et al., 2008). In addition, chronic saltwater exposure results in increased blood flow to the gland and changes in the innervation patterns of the tissue (Franklin and Grigg, 1993; Cramp et al., 2007). Very little is known about the cellular ion transport processes operating in the salt glands of crocodiles, nor is there much data pertaining to long-term changes in salt glands as a consequence of prolonged saltwater exposure. In the present study we sought to investigate how NKA responds to prolonged SW acclimation in the salt glands of juvenile *C. porosus* and to determine whether increases in salt gland secretory capacity correlate with increases in the activity and/or abundance of NKA in salt gland secretory cells. We hypothesised that like many other vertebrate salt glands, saltwater acclimation would result in an increase in NKA activity, abundance and gene expression which would serve to maximise the overall secretory capacity of the tissue.

MATERIALS AND METHODS

Animal husbandry

All experiments were carried out with the approval of the University of Queensland Animal Welfare Unit (permit numbers SIB/257/05/ARC/URG and SIB/186/06/ARC/URG) and Queensland Parks and Wildlife Service (permit no. WISP00993703).

Estuarine crocodiles (*C. porosus* Schneider 1801) were obtained from Fleays Wildlife Park (West Burleigh, QLD, Australia) as eggs and were incubated in a Clayson IM 1000 incubator (Axyos, Brendale, QLD, Australia) at 30°C in plastic containers covered in moist vermiculite. Upon hatching, all animals were held in 1000 l plastic Nally bins containing 20 l of heated (30±2°C) freshwater (FW). The crocodiles were fed weekly on a mixture of live crickets and thawed neonate mice. Once all animals were feeding well (~2 weeks) they were randomly assigned to treatment groups. Controls (N=6) remained in FW and saltwater-acclimated animals (N=6) were placed into 10% seawater (SW) made using commercially available artificial sea salt (Aquasonic P/L, Wauchope, NSW, Australia). Over the space of 2 weeks, the salt concentration was gradually increased to 70% that of SW (24–25‰ salinity). Water in the holding tanks was changed twice a week. Animals remained in these treatments for 6 months. Animals were fasted for 3–7 days before being killed by an overdose of sodium pentobarbital ('Thiobarb' Jurox, Rutherford, NSW, Australia) administered *via* the cervical sinus (Cramp et al., 2008). Salt glands were immediately dissected out from the tongue and placed into cold air-saturated crocodile Ringer solution (116 mmol l^{-1} NaCl, 4 mmol l^{-1} KCl, 2 mmol l^{-1} $CaCl_2$, 2 mmol l^{-1} $MgCl_2$, 15 mmol l^{-1} glucose, 5 mmol l^{-1} sodium pyruvate and 10 mmol l^{-1} Hepes-Na salt; osmolarity 300 mosmol l^{-1}, pH 7.6 adjusted with HCl or NaOH).

Tissue respiration

In vitro salt gland respiration was measured using a Strathkelvin Instruments (North Lanarkshire, Scotland, UK) Mitocell S200 microrespirometry system comprising a 782 oxygen meter, a 1302 oxygen electrode and an MT200 respirometer. Two to three small (<0.5 mm thick by 1 mm^2) slices of salt gland tissue were placed into a 10 mm×5 mm nylon mesh biopsy bag. The bag was placed into a beaker containing crocodile Ringer solution at room temperature bubbled continuously with air and allowed to equilibrate for 15 min. The bag was then placed into an MT200 microrespirometer containing a magnetic stir bar and 1 ml of air-saturated crocodile Ringer solution at 25°C. The chamber was sealed and the rate of oxygen consumption by the tissue in the chamber was recorded continuously over a period of 2 h or until the partial pressure of oxygen in the chamber had dropped by 50%. At the end of this period the chambers were opened and the Ringer solution replaced with fresh air-saturated Ringer solution containing 1 mmol l^{-1} ouabain. The chamber was once again sealed and the rate of oxygen consumption measured over 2 h. Preliminary trials were conducted during which time it was established that the rate of oxygen consumption by the isolated salt gland sections remained reasonably constant for more than 4 h. At the completion of the trial, tissue pieces were removed from the nylon mesh bags, blotted dry, weighed and frozen at –20°C for later determination of DNA content. Prior to the commencement and at the end of each trial, the rate of background oxygen consumption in the chamber (from contaminants and the electrode) in the absence of any tissue was recorded and this mean rate subtracted from the tissue rates. In order to minimise bacterial contamination of the chamber, chambers were cleaned prior to trials with 70% ethanol and the chamber Ringer solution was filtered through 0.2 µm Millipore syringe filters. Metabolic rate was determined using inbuilt functions of the Strathkelvin 782 meter normalised to both tissue mass and DNA content (see below). The proportion of total tissue oxygen consumption associated with NKA activity was determined by subtracting the rate of oxygen consumption in the presence of ouabain from that measured in the absence of ouabain.

Measurement of nucleic acid content

Total genomic DNA was extracted from salt gland tissues using a commercially available genomic DNA extraction kit (PureLink™ Genomic DNA Mini Kit, Invitrogen, Sydney, NSW, Australia). DNA concentration was determined fluorometrically (Qubit, Invitrogen).

NKA activity

NKA activity was measured using a previously described method (McCormick, 1993) whereby the ouabain-sensitive hydrolysis of ATP was coupled through the action of pyruvate kinase and lactate dehydrogenase to the oxidation of NADH, which was measured spectrophotometrically. ATP is regenerated during this process and the accumulation of ADP is equimolar to the oxidation of NADH. Approximately 50 mg of salt gland tissue was lightly macerated with a scalpel blade and then placed into 100 µl of ice-cold SEI buffer (150 mmol l^{-1} sucrose, 10 mmol l^{-1} EDTA and 50 mmol l^{-1} imidazole, pH 7.3), snap frozen in liquid nitrogen and stored at –80°C. Five to 10 min before the assay was started, the tissue was rapidly thawed, and homogenised on ice with an Eppendorf micropestle in 50 µl of ice-cold SEID buffer (150 mmol l^{-1} sucrose, 10 mmol l^{-1} EDTA, 50 mmol l^{-1} imidazole and 0.5% sodium deoxycholate, pH 7.3) for 60 s. The homogenised sample was then centrifuged at 5000 ***g*** for 30 s to pellet the insoluble material. A 10 µl sample of homogenate was added to each of four wells of a cold 96-well plate and then 200 µl of assay mixture containing 3 U ml^{-1} lactate dehydrogenase, 3.75 U ml^{-1} pyruvate kinase, 2.1 mmol l^{-1} phosphoenolpyruvate, 0.5 mmol l^{-1} ATP, 0.16 mmol l^{-1} NADH, 50 mmol l^{-1} imidazole, 47 mmol l^{-1} NaCl, 2.6 mmol l^{-1} $MgCl_2$ and 10.5 mmol l^{-1} KCl, pH 7.3 at 25°C was added to the first two wells and 200 µl of the same assay mixture plus 0.5 mmol l^{-1} ouabain was added to the remaining two wells.

The absorbance at 340 nm was measured every minute for 10 min in a multiwall plate reader (DTX 880 Multimode Detector, Beckman

Coulter, Gladesville, NSW, Australia). The linear rate of NADH disappearance from 2 to 10 min was determined and the NKA activity was calculated as the difference in ATP hydrolysis in the absence and presence of ouabain expressed as μmol ADP mg^{-1} protein h^{-1}. An ADP standard curve (from 0 to 20 nmol) was generated to convert absorbance values to ADP concentration. Protein concentration of the homogenate was determined flurometrically (Qubit, Invitrogen, Sydney, NSW, Australia).

Immunohistochemistry

The distribution of NKA protein in crocodile salt glands was examined using immunohistochemistry. Salt gland tissue pieces (3 mm^3) removed from the tongues of crocodiles from each treatment group after they had been killed were placed into 10 volumes of cold Zamboni's fixative (Sheehan and Hrapchak, 1980) for 24 h. The fixative was removed and the tissues washed in 3×2 min changes of 70% ethanol. Tissue pieces were then dehydrated and embedded in paraffin wax (Histoplast, Thermo Fisher Scientific, Sydney, NSW, Australia). Transverse sections of salt glands approximately 6 μm thick were placed onto poly-L-lysine-coated glass slides. Sections were allowed to dry overnight before being de-paraffinised in xylene and rehydrated. Sections were then washed in washing buffer (0.01 mol l^{-1} PBS, 0.05% Tween-20, pH 7.2; 3×2 min washes) and blocked at room temperature in normal goat serum (2% goat serum, 1% BSA, 0.1% cold fish skin gelatin, 0.1% Triton X-100, 0.05% Tween-20 and 0.05% sodium azide in 0.01 mol l^{-1} PBS, pH 7.2) for 30 min. Endogenous avidin and biotin activity was then blocked for 15 min each (0.001% in 0.01 mol l^{-1} PBS). The NKA primary antibody, α5, developed by D. M. Fambrough, was obtained from the Developmental Studies Hybridoma Bank developed under the auspices of the NICHD and maintained by The University of Iowa, Department of Biological Sciences (Iowa City, IA, USA). Primary antibody was diluted 1:1000 in 1% BSA, 0.1% cold fish skin gelatin and 0.05% sodium azide in 0.01 mol l^{-1} PBS, applied to sections and incubated in a moist chamber overnight at 4°C. Sections were then washed in washing buffer, blocked for 10 min in 3% H_2O_2 in 0.01 mol l^{-1} PBS and incubated in secondary antibody [B7264 biotinylated anti-mouse IgG (whole molecule); Sigma Aldrich, Sydney, NSW, Australia] diluted 1:500 in PBS for 30 min at room temperature. Sections were then incubated in extravidin–horseradish peroxide conjugate (1:400 in PBS) for 30 min after which time the chromogen (3,3′-diaminobenzidine, DAB, enhanced liquid substrate system for immunohistochemistry) was applied. The chromogen took 3 min to develop fully, after which sections were washed in distilled water to halt the reaction. Sections were then counterstained in 1:5 dilution of Gills Hematoxylin solution in water for 30–60 s. Sections were then washed in distilled water for 5 min and dehydrated in ethanol, cleared in xylene substitute and mounted in DPX medium (Proscitech, Thuringowa, QLD, Australia). Sections were viewed with an Olympus BH-2 microscope and digital images captured with a Leica DCF280 digital firewire camera (QLab, Brisbane, QLD, Australia). Appropriate controls (i.e. no primary or no secondary antibody applied) were performed to ensure there was no non-specific binding of secondary antibody or chromogen to tissues.

Images were imported into the software package SigmaScan™ (Cranes Software International, Melbourne, VIC, Australia) and analysed for total area occupied by NKA-containing cells and intensity of staining per unit area of stained tissue. An area of connective tissue surrounding the secretory tubules and containing haematoxylin-stained nuclei but no chromogen was used to create an average 'background level' from which increased intensity as a result of chromogen intensity could be established.

Western blotting

NKA protein abundance in salt gland tissues of FW- and SW-acclimated crocodiles was compared by western blotting. Salt gland tissue was collected from animals at the time of killing and snap frozen in liquid nitrogen. Tissues were then stored at –80°C until required. NKA-containing membrane fractions were prepared following previous methods (Choe et al., 2004). Frozen tissues were rapidly pulverised between two sheets of aluminium foil and immediately transferred into 100 μl cold homogenisation buffer (250 mmol l^{-1} sucrose, 30 mmol l^{-1} Tris, 1 mmol l^{-1} EDTA, 100 μg ml^{-1} phenylmethylsulfonyl fluoride (PMSF) and 5 mg ml^{-1} protease inhibitor cocktail), and homogenised briefly with an Eppendorf micropestle. Samples were then centrifuged at 1200 ***g*** for 15 min to pellet the cell debris. The supernatant was removed and centrifuged for 25 min at 23 000 ***g***. The resulting pellet was re-suspended in 50 μl of 50% modified Laemmli buffer (1.21 mol l^{-1} Tris, 10% glycerol and 0.4% SDS) in homogenisation buffer. The sample was vortexed lightly and centrifuged at 16 000 ***g*** for 15 s to pellet any undissolved material. Because of small starting tissue amounts, a 10 μl aliquot from each membrane fraction per animal within a treatment group was removed and combined together. This sample was mixed thoroughly and a 1 μl aliquot was removed for protein quantification. Total protein was quantified flurometrially (Qubit, Invitrogen).

A 1 μg sample of total membrane protein (FW and SW homogenates in alternating lanes) was loaded together with 4 μl NuPAGE LDS Sample Buffer (Invitrogen) and 1 μl of NuPAGE Reducing Agent (10×; Invitrogen). Samples were heated to 70°C for 10 min and then loaded into 3–8% NuPAGE Novex Tris-Acetate Mini gels (Invitrogen) and run at 150 V for 1 h. Protein samples were subsequently transferred to 0.45 μm Invitrolon PVDF membranes. Membranes were rinsed with distilled water, air dried and stored at 4°C until stained.

Western blot staining was performed using the Western Breeze Chromogenic kit (Invitrogen) which contained all necessary reagents except primary antibody. The primary antibody (α5) was applied at a dilution of 1:2500 for 1 h at room temperature. Following staining, membranes were washed in distilled water and allowed to dry at room temperature. Blots were then converted to digital images with a Canon flat bed scanner and analysed using the software package LabImage 1D 2006 Professional (www.labimage.com). Relative protein abundance was calculated by comparing the density of bands from FW-acclimated crocodile salt gland tissue homogenate with that from SW-acclimated animals. A total of four comparisons were made and the density of bands from FW-acclimated animals was set at 100%.

Peptide sequencing using LC-MS/MS

In order to confirm the identity of the protein band identified using the α5 antibody, peptide fragments from immunoreactive bands were sequenced by the Molecular and Cellular Proteomics Mass Spectrometry Facility (MCPMSF) in the Institute for Molecular Bioscience (IMB) at The University of Queensland (Brisbane, QLD, Australia) using liquid chromatography–mass spectrometric analysis (LC–MS/MS) as described in detail elsewhere (Kiel et al., 2007). Digests were analysed in LC–MS/MS mode for identification. Using a locally stored copy of Mascot (version 1.9) search engine (www.matrixscience.com), product ion data were searched against the publicly available NCBI non-redundant protein database (www.ncbi.nlm.nih.gov), allowing for cross-species protein identification.

NKA gene expression

Crocodile NKA gene sequencing

Tissue pieces collected from animals post-killing (N=3 per treatment) were rapidly snap frozen in liquid nitrogen and stored at –80°C. RNA from tissue fragments was extracted using a commercially available RNA extraction kit with inbuilt DNAase treatment (Arum Total RNA Fatty and Fibrous tissue extraction kit; Bio-Rad, Gladesville, NSW, Australia). RNA yield and quality were assayed by spectrometry (i.e. the ratio of absorbance at 260 nm to absorbance at 280 nm; Beckman Coulter DU800) and visually by 1.8 g 100 ml^{-1} agarose gel electrophoresis. An aliquot of RNA from one animal from each treatment group was used to generate cDNA. A fixed amount of total RNA (2 μg) was used in each cDNA reaction. The RNA was reverse transcribed into cDNA using the iScript (Bio-Rad) protocol (with random hexamers). Contaminating RNA was eliminated by incubation of the product with 0.5 μl of RNase H for 20 min at 37°C. The samples were PCR cleaned and eluted using the ChargeSwitch-Pro PCR Clean-up Kit (Invitrogen).

To identify the closest match, the human reference protein sequence for the α-subunit of the NKA gene (NM_000701) and the housekeeping gene β-actin (NM_001101), were used as a target to identify similar sequences in GenBank using the basic local alignment search tool BLASTp. We did not use an exhaustive gene identification approach to identify NKA α-subunit variants and as such it is possible that other isoforms or transcript variants may exist in the salt gland tissue. NKA degenerate primers were designed on the basis of conserved motifs in the corresponding protein sequences from five organisms (*Mus musculus* NP_659149, *Gallus gallus* NP_990852, *Anas platyrynchos* AAO42613, *Xenopus laevis* U49238 and *Squalus acanthias* CAG77578) which were aligned using Vector NTI software (Invitrogen) using the default settings. Degenerate primer sequences (5′–3′) were as follows: NKA forward: GAYCCWCCYCGWGCTGCTGT; NKA reverse: CCACCABSTNGGYTTGAGBGG. The amplicon size was 1169 bp.

β-actin degenerate primers were designed on the basis of conserved motifs in the corresponding protein sequences from five organisms (*M. musculus* NP_031419, *G. gallus* NP_990849, *Cynops ensicauda* BAC81772, *X. laevis* O93400 and *Danio rerio* AAB97964) which were aligned using Vector NTI software using the default settings. Degenerate primer sequences (5′–3′) were as follows: β-actin forward: TGGGAYGAYATGGARAAGATCTGG; β-actin reverse: CCACATCTGCGTGAAGGTGGA. The amplicon size was 811 bp.

The crocodilian NKA and β-actin cDNAs were amplified using standard PCR in 60 μl reactions (iTaq DNA polymerase, Bio-Rad). The stringency of the reaction was adjusted for the degenerate primers by lowering the annealing temperature from 60°C to 50°C. The amplicon was identified by size after 1% agarose gel electrophoresis and gel extracted (Freeze and Squeeze kit, Bio-Rad). The purified DNA was then submitted to the Australian Genome Research Facility (Brisbane, NSW, Australia) for sequencing using both the forward and reverse degenerate primers. Both sequenced gene fragments have been lodged with GenBank [NKA, 1069 bp partial coding sequence (cds), accession number: FJ644938; β-actin, 749 bp partial cds, accession number: GQ847622].

Gene expression

The cloned *C. porosus* sequence was used as the template to design specific 100–200 bp amplicons for quantitative PCR. All non-degenerate primer design was performed using OligoPerfect Designer software (Invitrogen), with acceptance of the default settings and optimisation for quantitative PCR. Gene-specific primer sequences (5′–3′) were as follows: NKA forward: GGA-ACCCCAAGACAGACAAA; NKA reverse: AAGCAAGGA-AGATGGCAGAA. Amplicon was 141 bp. β-actin forward: GTGCCCATCTACGAGGGTTA; β-actin reverse: TCTCAGC-TGTGGTGGTGAAG. Amplicon was 131 bp.

Quantitative RT-PCR was performed using Superscript III Platinum SYBR Green One-step kit (Invitrogen) using RNA as the input template. qRT-PCR amplification mixtures (12.5 μl) contained 100 pg RNA, 2× SYBR Green Reaction Mix (6.25 μl), 10 μmol l^{-1} forward and reverse primer (0.25 μl each) and Superscript III RT/Platinum Taq Mix (0.25 μl). Reactions were run on a sequence detector (MiniOpticon, Bio-Rad) using cycling parameters recommended in the qRT-PCR kit. Each assay (in triplicate) included a no-template control and a no-RT control. All PCR efficiencies were >90% and all the assays produced unique dissociation curves. MJ Opticon 3 software (version 3.1.32, Bio-Rad) results were exported as tab-delimited text files and imported into Microsoft Excel for further analysis. The expression of each gene was quantified relative to the expression of the housekeeping gene, β-actin, using the ΔCT method.

Reagents and chemicals

All reagents were purchased from Sigma Aldrich unless otherwise specified and all were of laboratory grade or higher.

Statistics

All data were compared statistically with t-tests, or paired t-tests for *in vitro* tissue respiration data, with α set at 0.05. All statistical calculations were performed using the statistical program SigmaStat 3.0^{TM} (Cranes Software International).

RESULTS

Salt gland oxygen consumption rate

In vitro metabolic rates of salt gland tissue segments from FW- and SW-acclimated *C. porosus* were compared in the absence and presence of the NKA-specific inhibitor ouabain to determine the relative contribution of NKA to the metabolic rate of the tissue. The metabolic rate of salt gland tissues in the absence of ouabain was not significantly different between FW- and SW-acclimated animals irrespective of whether data were normalised to tissue mass (P=0.945, t=0.071, d.f.=10; Fig. 1A) or DNA content (P=0.1207, t=1.696 d.f.=10, Fig. 1B). The incubation of tissues slices in 1 mmol l^{-1} ouabain resulted in a marked depression (approximately 50%) of metabolic rate (FW acclimated: P=0.019, t=3.409; d.f.=5; SW acclimated: P=0.008, t=4.316, d.f.=5; Fig. 1A); however, there was no significant difference in the proportion of total oxygen consumption rate associated with NKA activity in the salt gland tissues of FW- and SW-acclimated animals (P=0.372, t=0.934, d.f.=10).

NKA activity

There was no significant difference between the specific activity of the NKA enzyme in salt gland tissues from FW- and SW-acclimated crocodiles (P=0.653, t=0.463, d.f.=10; Fig. 2).

Peptide sequence identification

Analysis of trypic digests of immunoreactive protein bands by tandem mass spectroscopy revealed several matches with sodium/potassium-transporting ATPase α1 subunit peptides from species including mouse (*M. musculus*, Q8VDN2), chicken (*G.*

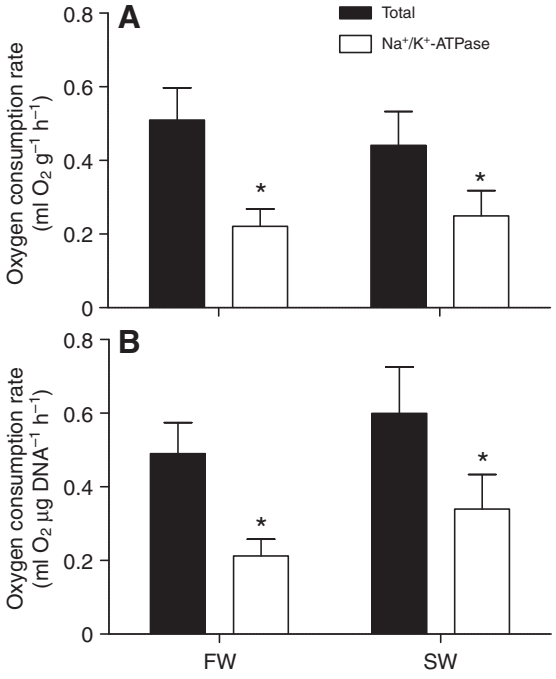

Fig. 1. *In vitro* oxygen consumption rates normalised to tissue mass (A) and DNA content (B) of salt gland slices from *Crocodylus porosus* juveniles following prolonged acclimation in freshwater (FW) and saltwater (SW) environs (filled bars). Open bars show the metabolic contribution of Na^+/K^+-ATPase (NKA) activity to the *in vitro* rate of oxygen consumption in salt gland slices, again normalised to tissue mass (A) and DNA content (B). Asterisks indicate significant differences between total oxygen consumption rate and ouabain-treated tissue oxygen consumption rate (P<0.05). Data are presented as means + s.e.m. (N=6 in each treatment).

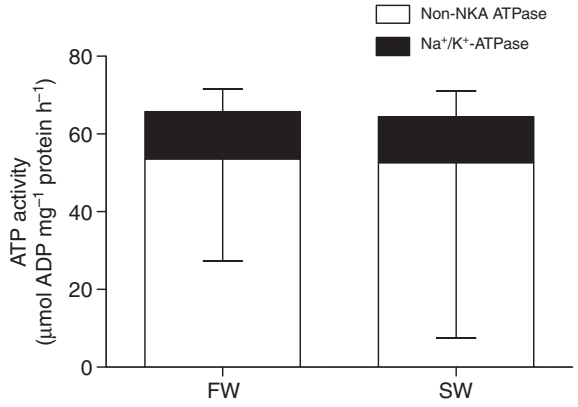

Fig. 2. Specific activity of NKA from salt gland secretory cells in the salt glands of FW- and SW-acclimated juvenile *C. porosus*. Data are presented as means ± s.e.m. (N=6 in each treatment).

gallus, P09572) and frog (*X. laevis*, Q92123), confirming that the α5 antibody was binding to the NKA protein in crocodile tissues.

NKA distribution

NKA distribution was visualised using immunohistochemistry. The α5 antibody localised primarily to the secretory tissue within the salt gland lobes (Fig. 3A,B); there was little or no non-specific binding by either the primary or secondary antibodies.

NKA signal was restricted to the basolateral membrane of the secretory cells. There was very little signal present in the apical membranes (Fig. 3C,D). Although all secretory cells in the salt gland lobes were immunoreactive to the NKA antibody, there was an obvious regional staining pattern, with cells along the periphery of the tissue being less intensely stained than those towards the centre of the lobe. This pattern was evident in tissues from both treatments, but was particularly apparent in tissues from SW-acclimated *C. porosus* (Fig. 3D).

There was a statistically significant difference between the overall NKA staining intensity per unit area of salt gland lobes from SW-acclimated crocodiles relative to those from FW-acclimated crocodiles (P=0.029, t=–2.66, d.f.=8; Fig. 3E).

NKA abundance

NKA abundance was estimated using western blotting. Antibody α5, specific for the NKA α-subunit, recognised a single band of approximately 98 kDa (Fig. 4). Blots from SW-acclimated *C. porosus* indicated a significant 2-fold increase in the amount of NKA per mg of loaded protein relative to that from FW-acclimated crocodiles (P<0.001, t=–17.43, d.f.=6; Fig. 4).

NKA gene expression

No reptile genome has been fully sequenced. Consequently, degenerate primers were designed to amplify >200 bp of the *C. porosus* sequence. The nucleotide sequence returned from *C. porosus* genes sequenced in this study showed the highest similarity (>90%) to amphibian (*X. laevis*) and avian sequences (*A. platyrynchos*) and was typically around 87–90% similar to that of other vertebrates.

NKA expression was examined relative to the housekeeping gene β-actin. β-actin expression was unaffected by acclimation treatment, and hence served as an appropriate reference gene. SW acclimation resulted in a 3-fold relative increase in NKA gene expression in *C. porosus* salt glands (Fig. 5); however, due to the small sample sizes, this did not reach statistical significance (P=0.06, t=2.551, d.f.=4).

DISCUSSION

Using a specific antibody directed against the α-(catalytic) subunit of NKA, we were able to demonstrate that NKA was present throughout the salt glands of *C. porosus* hatchlings reared in both FW and SW. NKA signal was present in the basolateral membranes of most cells but was only faintly detectable in apical membranes and then only in a minority of cells. There was little evidence of NKA in the connective tissue or blood vessels. The distribution of NKA within the salt glands of *C. porosus* is largely consistent with that of other vertebrate extra-renal salt-secreting tissues (Abel and Ellis, 1966; Ellis and Goertemiller, 1974; Thompson and Cowan, 1976; Eveloff et al., 1979).

In *C. porosus*, NKA staining intensity was clearly greater in the secretory cells which occurred in the middle of the salt gland lobes, with those in the immediate periphery having a visibly reduced staining intensity. This pattern of distribution was evident in both FW- and SW-acclimated crocodile salt glands. This regional staining pattern may reflect differential patterns of secretory cell activity throughout the lobe. Blood flow within the salt glands is from the centre of the gland to the periphery, counter to that of secretion. Hence NKA density may be greater in cells towards the centre of the gland because of their contact with blood containing the highest concentration of salt (Franklin and Grigg, 1993). A similar regional distribution of enzyme activity has been described in both marine

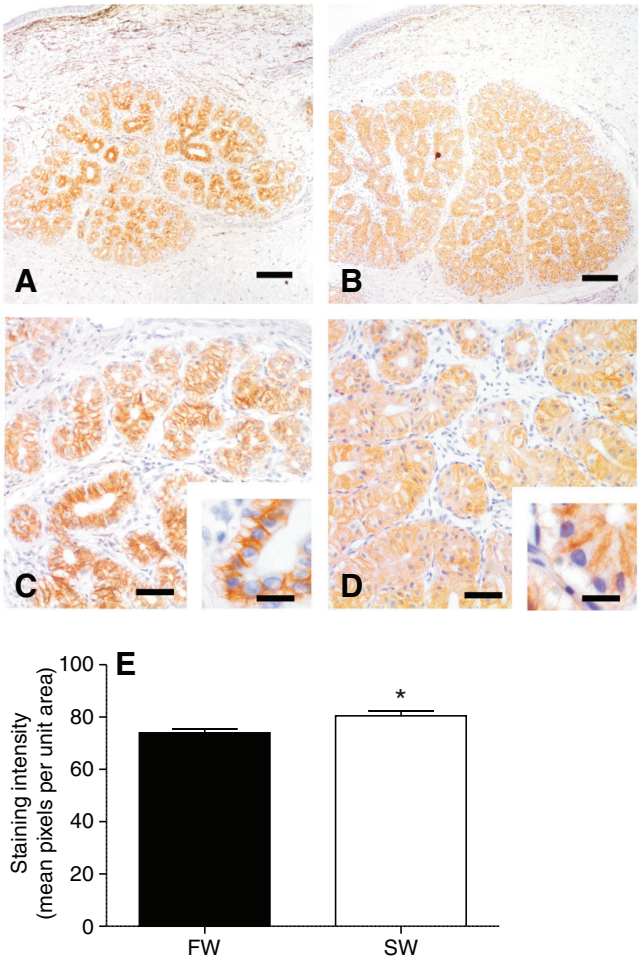

Fig. 3. Immunolocalisation of NKA α-subunit in the salt gland secretory cells of FW-acclimated (A,C) and SW-acclimated (B,D) *C. porosus* juveniles. Scale bars 150 μm (A,B), 60 μm (C,D) and 35 μm (insets). (E) There was a slight increase in the mean lobe staining intensity of tissues from SW-acclimated crocodiles. Asterisk indicates significant difference between treatments (P<0.05). Data are presented as means + s.e.m. (N=6 in each treatment).

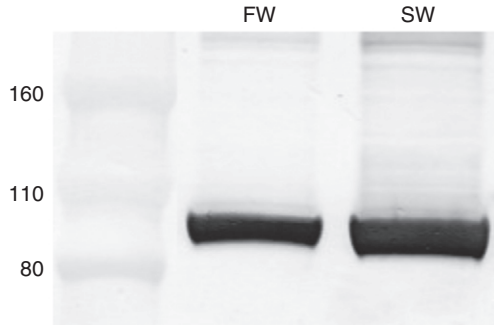

Fig. 4. Western blots showing a difference in the relative abundance of NKA α-subunit in salt glands from FW- and SW-acclimated *C. porosus*. There was a 2-fold increase in the abundance of the α-subunit in the salt glands of SW-acclimated *C. porosus*.

turtle and marine bird salt glands, where the vascular drainage patterns mirror those seen in *C. porosus* salt glands (Ellis et al., 1963; Abel and Ellis, 1966).

The mean NKA staining intensity per salt gland lobe was greater (~8%) in SW-acclimated *C. porosus* relative to FW-acclimated ones, suggesting that there was an increase in the density of NKA in the salt glands of SW-acclimated crocodiles. Indeed, analysis of western blots demonstrated a 2-fold increase in the abundance of NKA α-subunits in SW-acclimated crocodiles consistent with an increase in α-subunit mRNA abundance. An increase in the abundance of NKA protein subunits within avian salt glands from acutely salt loaded ducks is well documented and this increase is responsible for the marked increase in NKA activity typical of avian salt glands following acute salt loading (Hildebrandt, 1997). However, in *C. porosus*, an increase in the functional activity of NKA was not correlated with an increase in the abundance of the NKA α-subunit. In *C. porosus* juveniles chronically acclimated to a SW environment, specific NKA activity was not different from that of FW-acclimated animals. This suggests the abundance of the NKA α-subunit does not necessarily reflect NKA activity in SW-acclimated juvenile *C. porosus*.

The activity of the NKA pump often accounts for a considerable proportion of the total oxygen consumption rate of many highly active tissues. The *in vitro* oxygen consumption rate of salt gland tissue slices was measured to determine both the energy costs associated with chronic SW acclimation and the relative energy costs associated with maintaining NKA activity in the tissue. Consistent with a previous study (Cramp et al., 2008), chronic SW acclimation had no impact on the *in vitro* mass-specific metabolic rate of salt gland tissue slices. Used as an indirect measure of salt gland activity, the rate of oxygen consumption by isolated salt gland tissue slices from SW-acclimated crocodiles suggests that there was no apparent increase in cellular activity levels from that seen in FW-acclimated crocodiles, despite an increased capacity for salt secretion (Cramp et al., 2008). The absence of any increase in the rate of oxygen consumption by salt gland slices from SW-acclimated *C. porosus* contrasts with results from the avian literature which show that salt loading correlates with a marked increase in tissue oxygen consumption rates (Hootman and Ernst, 1980). In avian salt gland models, isolated secretory cells from salt glands of salt-stressed ducks were almost 50% more metabolically active than those from naïve ducks (Hootman and Ernst, 1980). Contributing to a large proportion of the increase in metabolic rate of the tissue from salt-stressed ducks is increased NKA activity (Hootman and Ernst, 1980). In FW-acclimated *C. porosus*, the activity of the NKA pump accounted for approximately 43% of the total oxygen consumption rate of the tissue. This figure was not significantly different for SW-acclimated animals (54%), suggesting that there is no difference in energy costs associated with NKA activity in tissues from SW-acclimated animals. These results are consistent with our earlier finding that in the salt glands of *C. porosus*, NKA activity, and therefore the energy costs associated with maintaining NKA activity within the tissue, is not affected by chronic SW acclimation.

The results from the present study raise interesting questions as to the role of NKA in salt secretion and the effect of long-term salt exposure on salt gland function in chronically SW-acclimated *C. porosus* juveniles. Given the remarkable degree of similarity in the morphology and function of salt glands from birds, other reptiles and elasmobranchs, which have evolved largely independently, we expected that NKA in the salt glands from *C. porosus* would respond to salt loading in much the same way as in other salt gland models. Why, then, does chronic SW acclimation not result in markedly

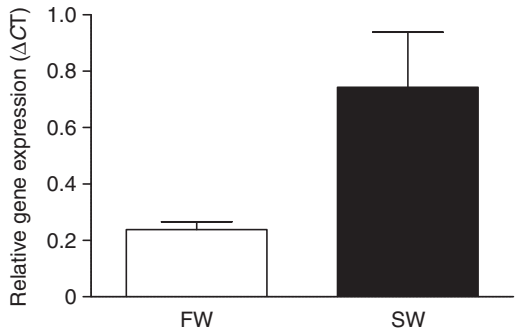

Fig. 5. NKA mRNA expression (*N*=3 per treatment) in the salt glands from *C. porosus* juveniles chronically exposed to either FW or SW. Absolute gene expression (ΔCT) was normalised to that of the housekeeping gene β-actin. Data are presented as means + s.e.m. (*N*=3 in each treatment).

elevated NKA activity levels in *C. porosus*? There are several potential reasons for this.

Firstly, it is possible that exposure to salt water alone is not sufficient to stimulate salt gland function to the extent seen in some marine birds and reptiles. Early work on the salt glands of sea snakes and terrapins suggested that increases in NKA activity, in particular, become apparent in SW-acclimated animals only after extensive artificial salt loading (Dunson and Dunson, 1975) because of a lack of need to drink seawater to maintain hydration. Earlier work suggested that *C. porosus* may not need to drink seawater (Taplin, 1984; Taplin, 1985) and therefore might only experience salt loading as a consequence of feeding. In a similar study, fasted dogfish *Scyliorhinus canicula* fed a meal of squid experienced a delayed and transient increase in NKA activity of the rectal gland (MacKenzie et al., 2002). In that study, NKA activity began to increase 3 h after the ingestion of the meal, reached a maximum (40-fold increase in NKA activity) at 9 h and completely returned to basal levels within 24 h of ingestion of the meal. In addition, NKA α-subunit mRNA abundance increased following squid ingestion; mRNA transcript abundance gradually increased over the first 2 days following feeding, peaked at 5 days (90% more than in controls), and at day 10 there was still 50% more transcript in the rectal glands of fed animals relative to fasted controls (MacKenzie et al., 2002). In the present study, animals were fed neonate mice, which have a Na^+ content within the range of diets naturally experienced by animals living in hypersaline environments (Grigg et al., 1986; Cramp et al., 2008). However, for the purposes of other experiments not reported here animals were killed several days after the ingestion of the last meal. Therefore it is possible that as in dogfish, NKA activity is transiently increased following feeding in *C. porosus* to accommodate the acute salt load, and subsequently activity declines. In the present study, the expression and abundance of NKA α-subunits were elevated at least 3–7 days post-feeding, which is again consistent with the dogfish study. In *C. porosus*, like *S. canicula*, the increased expression of NKA in the absence of a detectable increase in activity suggests that NKA activity may be modulated post-transcriptionally by as yet unknown regulatory factors.

Secondly, it is possible that NKA activity levels may have declined over time as a consequence of prolonged acclimation to SW environments. The majority of the existing literature pertaining to the cellular regulation of salt gland function in other animal models is focused on exposure of naïve animals to substantial but acute salt loads, which may last between a few hours and a few weeks. Very little information exists investigating the potential for long-term acclimation of salt glands to persistently high levels of salt loading. If initial exposure to seawater in juvenile *C. porosus* stimulates increases in NKA activity to the extent and manner seen in other salt gland models, it is possible that the associated energetic costs are such that the long-term maintenance of these might result in some acclimatory compensation. However, the acclimation of crocodile NKA activity following prolonged saltwater exposure would require the coordinated acclimation of other ion transport pathways (both active and passive). At present, we have no information relating to the activity and behaviour of other ion transport pathways in the salt glands of SW-acclimated *C. porosus*. More investigation into the regulation of ion transport pathways following SW acclimation is required before we can determine whether *C. porosus* can regulate the physiological plasticity of salt glands through the coordinated acclimation of numerous ion transport pathways.

The results from the present study indicate that NKA is present in the salt glands of *C. porosus* and that it is involved in the functional activity of the tissue. NKA is broadly distributed throughout the secretory cells, restricted largely to the lateral membranes. A large proportion of the total energy consumption of the tissue is attributable to the activity of NKA. However, chronic SW acclimation alone is not sufficient to stimulate NKA activity in the manner seen in other animal models. Despite this, NKA mRNA and protein abundance are greater in SW-acclimated animals, suggesting that post-transcriptional factors may regulate NKA activity. Whether these results reflect long-term SW acclimation or the consequence of more transient changes in NKA activity associated with feeding episodes remains unclear at this time. Future work is required to separate acute *versus* chronic changes in NKA activity and abundance as well as the role played by diet and feeding in stimulating NKA up-regulation in *C. porosus* salt glands.

ACKNOWLEDGEMENTS

We would like to thank Alun Jones of the Molecular and Cellular Proteomics Mass Spectrometry Facility (MCPMSF) within the Institute for Molecular Bioscience (IMB) at The University of Queensland for the LC-MSMS work, Inga De Vries and the Franklin lab volunteers for assistance with the husbandry of crocodiles and The David Fleay Fauna Centre for their donations of crocodile eggs. This project was funded by an Australian Research Council Discovery Grant and a University of Queensland Research Grant.

REFERENCES

Abel, J. H., Jr and Ellis, R. A. (1966). Histochemical and electron microscopic observations on the salt secreting lacrymal glands of marine turtles. *Am. J. Anat.* **118**, 337-357.

Bentz, C., Schwarz, M. and Hildebrandt, J. P. (1999). Cytosolic pH affects DNA-synthesis in nasal gland cells of osmotically stressed ducklings, *Anas platyrhynchos*. *Zoology* **102**, 10-17.

Bulger, R. E. (1963). Fine structure of the rectal (salt-secreting) gland of the spinydogfish, *Squalus acanthias*. *Anat. Rec.* **147**, 95-127.

Choe, K. P., O'Brien, S., Evans, D. H., Toop, T. and Edwards, S. L. (2004). Immunolocalization of Na^+/K^+-ATPase, carbonic anhydrase II, and vacuolar H^+-ATPase in the gills of freshwater adult lampreys, *Geotria australis*. *J. Exp. Zool.* **301**, 654-665.

Cramp, R. L., Hudson, N. J., Holmberg, A., Holmgren, S. and Franklin, C. E. (2007). The effects of saltwater acclimation on neurotransmitters in the lingual salt glands of the estuarine crocodile, *Crocodylus porosus*. *Regul. Pept.* **140**, 55-64.

Cramp, R. L., Meyer, E. A., Sparks, N. and Franklin, C. E. (2008). Functional and morphological plasticity of crocodile (*Crocodylus porosus*) salt glands. *J. Exp. Biol.* **211**, 1482-1489.

Dunson, M. K. and Dunson, W. A. (1975). Relation between plasma Na concentration and salt gland Na-K ATPase content in Diamondback Terrapin and Yellow-Bellied Sea Snake. *J. Comp. Physiol.* **101**, 89-97.

Dunson, W. (1968). Salt gland secretion in the pelagic sea snake *Pelamis*. *Am. J. Physiol.* **215**, 1512-1517.

Ellis, R. A. and Goertemiller, C. C., Jr (1974). Cytological effects of salt-stress and localization of transport adenosine triphosphatase in the lateral nasal glands of the desert iguana, *Dipsosaurus dorsalis*. *Anat. Rec.* **180**, 285-297.

Ellis, R. A., Delellis, R. A., Goertemiller, C. C. and Kablotsky, Y. H. (1963). Effect of a salt water regimen on development of salt glands of domestic ducklings. *Dev. Biol.* **8**, 286-308.

Evans, D. H. (2008). Teleost fish osmoregulation: what have we learned since August Krogh, Homer Smith and Ancel Keys. *Am. J. Physiol.* **295**, R704-R713.
Eveloff, J., Karnaky, K. J., Jr, Silva, P., Epstein, F. H. and Kinter, W. B. (1979). Elasmobranch rectal gland cell: autoradiographic localization of [^{3}H]ouabain-sensitive Na, K-ATPase in rectal gland of dogfish, *Squalus acanthias*. *J. Cell Biol.* **83**, 16-32.
Fletcher, G. L., Stainer, I. M. and Holmes, W. N. (1967). Sequential changes in the adenosinetriphosphatase activity and the electrolyte excretory capacity of the nasal glands of the duck (*Anas platyrhynchos*) during the period of adaptation to hypertonic saline. *J. Exp. Biol.* **47**, 375-391.
Franklin, C. E. and Grigg, G. C. (1993). Increased vascularity of the lingual salt glands of the estuarine crocodile, *Crocodylus porosus*, kept in hyperosmotic salinity. *J. Morphol.* **218**, 143-151.
Grigg, G. C., Taplin, L. E., Green, B. and Harlow, P. (1986). Sodium and water fluxes in free living *Crocodylus porosus* in marine and brackish conditions. *Physiol. Zool.* **59**, 240-253.
Hildebrandt, J. P. (1997). Changes in Na^+/K^+-ATPase expression during adaptive cell differentiation in avian nasal salt gland. *J. Exp. Biol.* **200**, 1895-1904.
Hootman, S. R. and Ernst, S. A. (1980). Dissociation of avian salt glands: separation procedures and characterization of dissociated cells. *Am. J. Physiol.* **238**, C184-C195.
Kiel, M., Josh, P., Jones, A., Windon, R., Hunt, P. and Kongsuwan, K. (2007). Identification of immuno-reactive proteins from a sheep gastrointestinal nematode, *Trichostrongylus colubriformis*, using two-dimensional electrophoresis and mass spectrometry. *Int. J. Parasitol.* **37**, 1419-1429.
Kirschner, L. B. (1980). Comparison of vertebrate salt-excreting organs. *Am. J. Physiol.* **238**, R219-R223.
Knight, C. H. and Peaker, M. (1979). Adaptive hyperplasia and compensatory growth in the salt glands of ducks and geese. *J. Physiol.* **294**, 145-151.
MacKenzie, S., Cutler, C. R., Hazon, N. and Cramb, G. (2002). The effects of dietary sodium loading on the activity and expression of Na, K-ATPase in the rectal gland of the European Dogfish (*Scyliorhinus canicula*). *Comp. Biochem. Physiol. B* **131**, 185-200.
McCormick, S. (1993). Methods for non-leathal gill biopsy and measurement of Na^+K^+ATPase activity. *Can. J. Fish. Aquat. Sci.* **50**, 656-658.
Piermarini, P. M. and Evans, D. H. (2000). Effects of environmental salinity on Na^+/K^+-ATPase in the gills and rectal gland of a euryhaline elasmobranch (*Dasyatis sabina*). *J. Exp. Biol.* **203**, 2957-2966.
Pillans, R. D., Good, J. P., Anderson, W. G., Hazon, N. and Franklin, C. E. (2005). Freshwater to seawater acclimation of juvenile bull sharks (*Carcharhinus leucas*): plasma osmolytes and Na(+)/K(+)-ATPase activity in gill, rectal gland, kidney and intestine. *J. Comp. Physiol. [B].* **175**, 37-44.
Schmidt-Nielsen, K. (1960). The salt-secreting gland of marine birds. *Circulation* **21**, 955-967.
Schmidt-Nielsen, K. and Fänge, R. (1958). Salt glands in marine reptiles. *Nature* **182**, 783-785.
Schmidt-Nielsen, K. and Kim, Y. (1964). The effect of salt intake on the size and function of the salt gland of ducks. *Auk* **81**, 160-172.
Scott, G. R., Richards, J. G., Forbush, B., Isenring, P. and Schulte, P. M. (2004). Changes in gene expression in gills of the euryhaline killifish, *Fundulus heteroclitus* after abrupt salinity transfer. *Am. J. Physiol.* **287**, C300-C309.
Sheehan, D. C. and Hrapchak, B. B. (1980). *Theory and Practice of Histotechnology*. St Louis: Mosby.
Shuttleworth, T. J. and Hildebrandt, J. P. (1999). Vertebrate salt glands: short- and long-term regulation of function. *J. Exp. Zool.* **283**, 689-701.
Taplin, L. E. (1984). Drinking of fresh water but not seawater by the Estuarine Crocodile (*Crocodylus porosus*). *Comp. Biochem. Physiol. A* **77**, 763-767.
Taplin, L. E. (1985). Sodium and water budgets of the fasted estuarine crocodile, *Crocodylus porosus* in sea water. *J. Comp. Physiol. B* **155**, 501-513.
Taplin, L. E. and Grigg, G. C. (1981). Salt glands in the tongue of the Estuarine Crocodile *Crocodylus porosus*. *Science* **212**, 1045-1047.
Taub, A. M. and Dunson, W. A. (1967). The salt gland in a sea snake (Laticauda). *Nature* **215**, 995-996.
Thompson, I. G. and Cowan, F. B. (1976). Localization of K^+-stimulated p-NPPase in the lachrymal 'salt' gland of *Malaclemys*, using cytochemical and autoradiographical techniques. *Cell Tissue Res.* **174**, 417-426.